

Supporting Information

Synthesis of In_2O_3 nanoparticle/ TiO_2 nanobelt heterostructures for near room temperature ethanol sensing

Yujie Li¹, Hongru Yang¹, Jian Tian*, Xiaolin Hu, Hongzhi Cui*

School of Materials Science and Engineering, Shandong University of Science and Technology,
Qingdao 266590, China.

Email: jiantian@sdust.edu.cn, cuihongzhi1965@163.com

¹ These authors contributed equally.

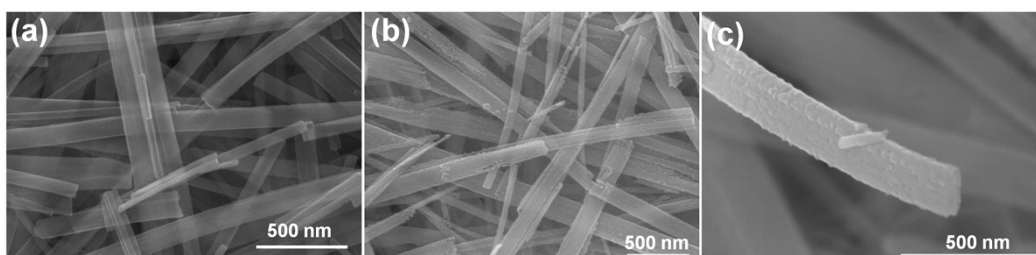


Figure S1. SEM image of (a) TiO_2 nanobelts and (b, c) surface-coarsened TiO_2 nanobelts.

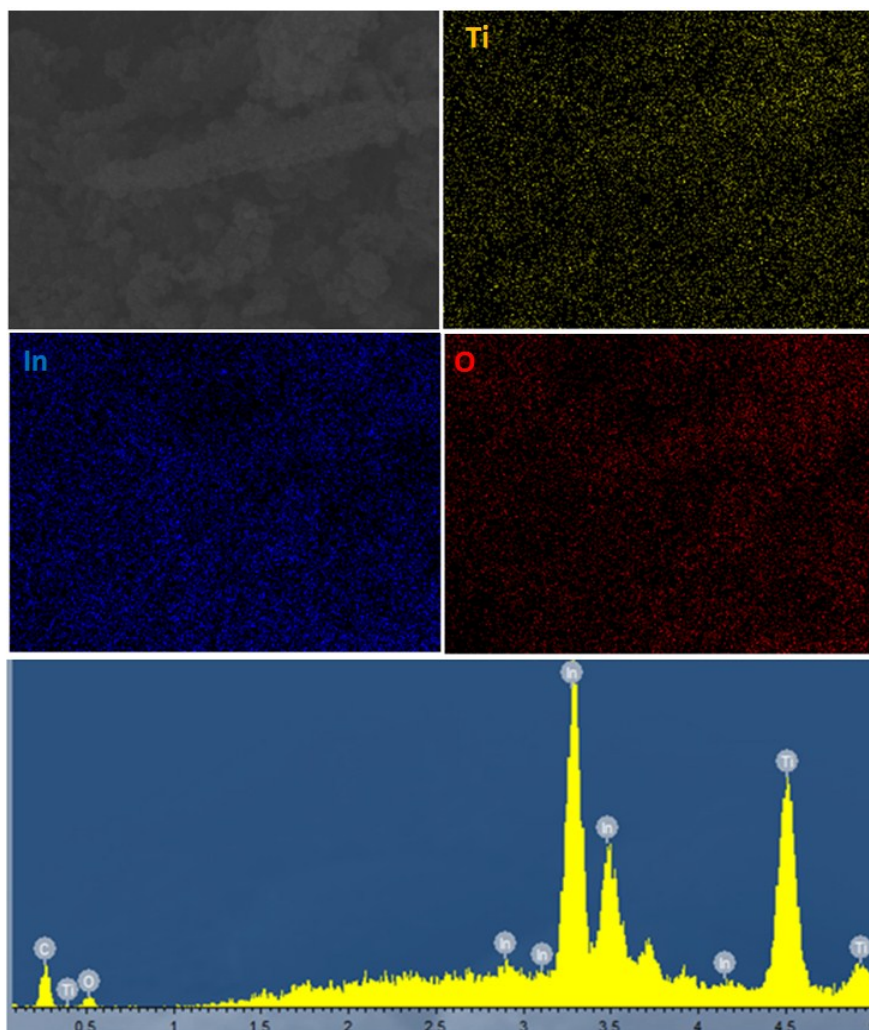


Figure S2. Elemental energy-dispersive X-ray spectroscopy (EDS) mapping of the obtained In_2O_3 nanoparticle/ TiO_2 nanobelt heterostructures (mole ratio 1:1).

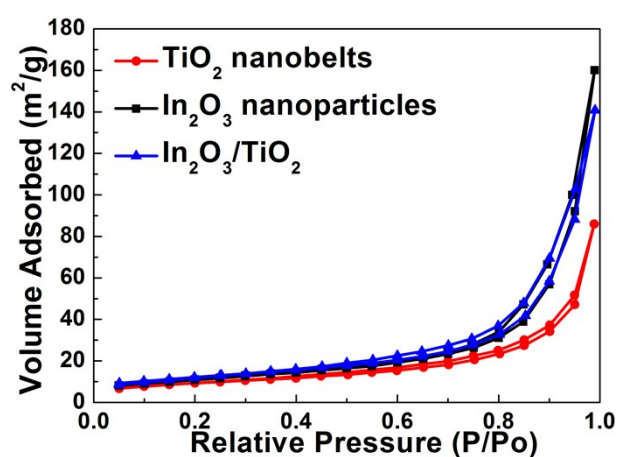


Figure S3. Nitrogen adsorption-desorption isotherms of TiO_2 nanobelts, In_2O_3 nanoparticles and In_2O_3 nanoparticle/ TiO_2 nanobelt heterostructures (mole ratio 1:1).

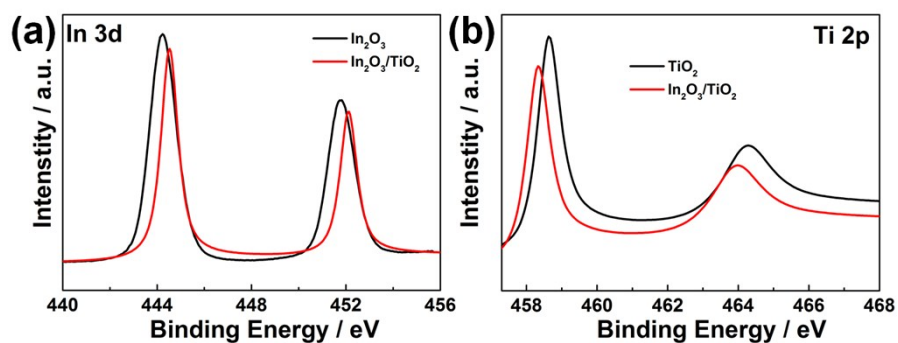


Figure S4. (a) In3d and (b) Ti2p core-level XPS spectra of the samples.

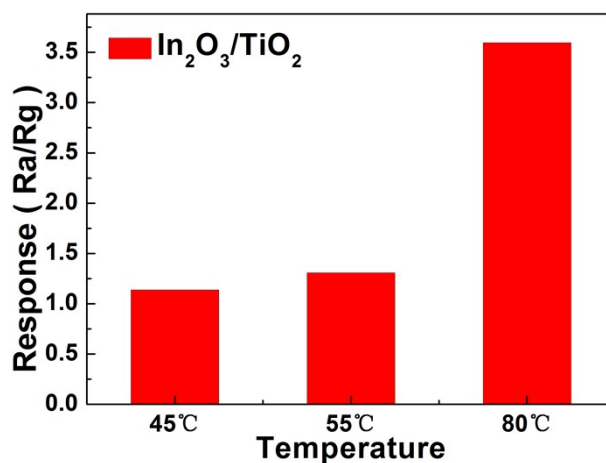


Figure S5. Response of ethanol vapor sensors based on In_2O_3 nanoparticle/ TiO_2 nanobelt heterostructures (mole ratio 1:1) upon exposure to 100 ppm of ethanol vapor at low operating temperature (45 °C, 55 °C and 80 °C).

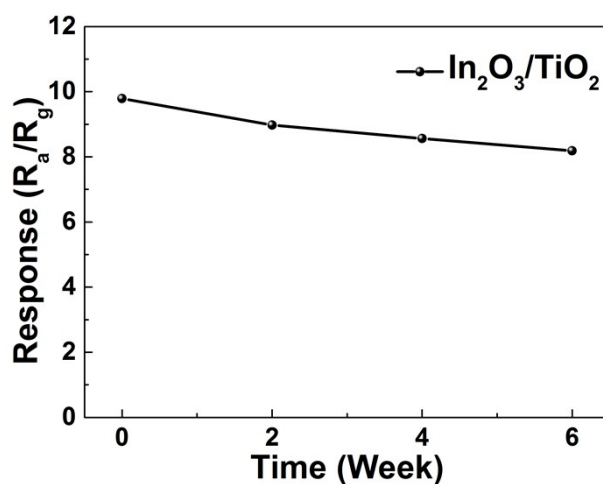


Figure S6. The sensing stability of the In_2O_3 nanoparticle/ TiO_2 nanobelt heterostructures (mole ratio 1:1) sensor to 100 ppm ethanol with respect to a low

temperature of 100 °C.

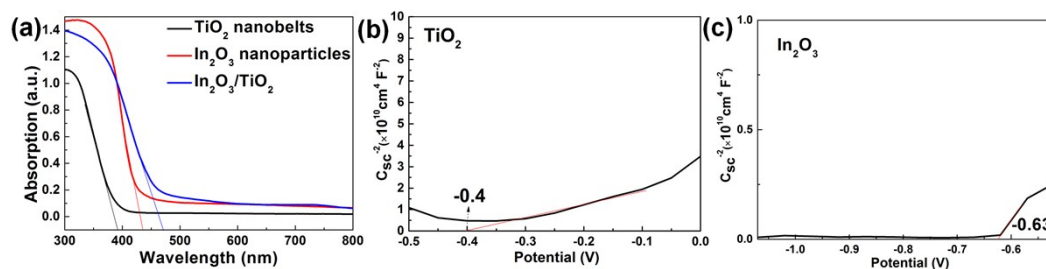


Figure S7. (a) UV-vis diffuse reflectance spectra of TiO₂ nanobelts, In₂O₃ nanoparticles and In₂O₃ nanoparticle/TiO₂ nanobelt heterostructures. Mott-Schottky plots of (b) TiO₂ nanobelts and (c) In₂O₃ nanoparticles collected at a frequency of 1000 Hz in dark.

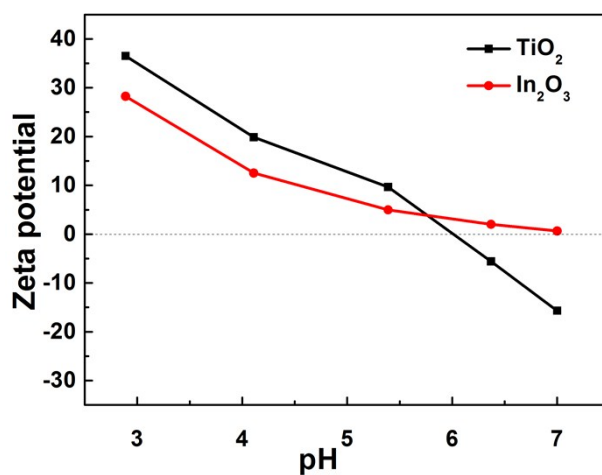


Figure S8. Zeta potentials of TiO₂ nanobelts and In₂O₃ nanoparticles in aqueous solution at different pH values.